Express Polymer Letters Vol.18, No.9 (2024) 950–961
Available online at www.expresspolymlett.com
https://doi.org/10.3144/expresspolymlett.2024.72

Research article

Microstructural phenomena in ground tire rubber (GTR) devulcanized *via* combined thermochemomechanical and microwave processes monitored by FTIR and DTGA assisted by other techniques

Xavier Colom[1*], *Mohammad Reza Saeb*[2], *Javier Cañavate*[1]

[1]Department of Chemical Engineering, Universitat Politècnica de Catalunya BarcelonaTech, Terrassa, Spain
[2]Department of Pharmaceutical Chemistry, Medical University of Gdańsk, J. Hallera 107, 80-416 Gdańsk, Poland

Received 14 May 2024; accepted in revised form 26 June 2024

Abstract. Analyzing rubber waste is crucial for value-added recycling, but the multitude of ingredients in vulcanized networks makes it challenging to characterize cross-linked rubbers. A combination of analytical techniques is usually required. In this study, two complementary characterization techniques, based on Fourier transform infrared (FTIR) spectroscopy and derivative thermogravimetric analysis (DTGA) were applied to analyze the structural, physical, and thermal behavior of ground tire rubber (GTR) samples devulcanized by two different processes. A set of samples was devulcanized by only microwaves (MW) while another set was treated with a combination of a thermochemomechanical (TM) process, which included the use of a devulcanization aid such as benzoyl peroxide, and microwaves. The combined technique proved to be more efficient in terms of the degree of devulcanization, significantly reducing the cross-linking density. However, the combined thermochemomechanical and microwave (TM/MW) devulcanization process resulted in greater degradation of the main rubber chains in the cross-linked network compared to the process using only microwaves.

Keywords: *FTIR, GTR, devulcanization, microwave, thermochemomechanical, DTGA, Horikx, chemomechanical*

1. Introduction

Approximately 3.6 million t of used tires are generated annually in the European Union (EU) [1]. As tires age, they gradually degrade, releasing a significant portion of their weight as very fine rubber dust into the environment. Besides this significant issue, the vast number of used tires also poses an environmental threat. Addressing this challenge requires a combination of sustainable recycling and upcycling strategies, aligned with the global shift towards achieving circular economy principles [2]. To effectively valorize these waste tires, it is important to reconsider and enhance the strategies for their recycling and reuse.

Currently, according to the final products obtained from discarded materials, like waste tires, the recycling processes can be classified into several categories. Primary recycling would be the reprocessing of a product, with scarce extra handling, into materials or goods with the same characteristics or comparable properties as the raw material from which it originated [3]. Secondary recycling is defined as the process in which these waste tires would be transformed into products that do not have similar or comparable properties to those of the original material. Tertiary recycling involves the decomposition of the elastomeric residue into smaller macromolecular structures, which can later be repolymerized into

*Corresponding author, e-mail: xavier.colom@upc.edu

new materials that could have properties different from those of the original elastomer. The tertiary recycling can be performed by pyrolysis, obtaining recovered carbon black (rCB), recovered steel, pyrolytic oil, and pyrolytic gas. It can also be achieved by devulcanization, where the crosslinked elastomeric structure of the tire is eliminated, allowing the resulting polymers to be revulcanized again in a new shape. Presently, this technique is being applied to certain types of elastomeric waste and ground tire rubber (GTR). There could also be a quaternary recycling, consisting of incineration. Considering the elastomeric part of the used tires is organic matter, the thermal energy released by its combustion (~32 MJ/kg) exceeds that of many fossil fuels, such as gas, fuel oil, or coal [4]. In the EU, approximately 38% of the used tire rubber is directed to energy recovery projects, such as thermal energy generation and use in cement plants [5].

Apart from special cases, devulcanization is a process in which a good balance between performance and environmental responsibility is achieved. The devulcanization process allows the rubber to be reused to generate a product like that of the original in terms of properties, where the environmental pollution would depend on the type of process used. Despite the implementation of several industrial solutions for devulcanization and the availability of devulcanized rubber on the market, enhancing the efficiency of the process and ensuring environmental protection remain ongoing challenges. Moreover, achieving widespread industrial-scale implementation represents a significant hurdle that researchers continue to address. In recent years, diverse rubber recycling methods have been described in the literature, with notable attention to mechanical processes (32%) [6–8], thermochemomechanical methods (6%) [9, 10], ultrasonic methods (4%) [11, 12], chemical processes (19.2%) [13–15], microwave techniques (25.8%) [16–20], cryogenic approaches (1.2%) [21], microbial solutions (2.7%) [22], and combined thermochemomechanical and microwave methods (9.9%) [23, 24], emphasizing application of sustainable approaches and technologies.

One of the great challenges encountered in ground tire rubber (GTR) devulcanization is the efficiency and general performance of the process [18, 23]. The vulcanization involves the creation of a crosslinked structure between the polymeric chains of the elastomer. These crosslinks are constituted by –S–S– bridges. The devulcanization process is directed to the breaking of these disulfide or polysulfidic links. Most devulcanization processes, when applied to a sample to break the di or polysulfide bonds, also act on the main polymeric chain breaking the macromolecules of the elastomer. This results in a decrease in the crosslinking degree and the degradation of the polymer. The microwave-based methods, because of the possibility of delivering very precise amounts of energy, are considered selective, being able to focus on disulfide bonds without acting too much on the –C–C– that constitutes the main polymeric chain.

Once one of the aforementioned devulcanization processes is selected, various methods would be available to analyze the outcome of the devulcanization process, such as determination of the crosslinking degree, measuring the sol fraction [%], or the selectivity coefficient (k) [25]. These methods lack the possibility of discerning between the breaking of the disulfide bonds and the –C–C– bonds. A loss in the crosslinking degree should occur, but there is no way of monitoring if the devulcanization has been initiated through a theoretically proper way, namely, with selective action on the disulfide bonds. To avoid this inconvenience, the use of the Horikx equations or Horikx plot or other analytical techniques such as Fourier-transform infrared spectroscopy (FTIR) has been recommended, allowing determining the microstructural and chemical changes taking place in a devulcanized sample. This is known for providing useful tools to assess the efficiency and intensity of the process and also the degradation that is produced in the elastomers [26]. For instance, Paulo *et al.* [27] analyzed the degree of devulcanization of styrene-butadiene rubber (SBR) by microwaves using inorganic salts and nitric acid through FTIR, finding that the presence of carbon black is relevant in the process and that some metallic ions decrease the sulfur crosslink content and promote the oxidation in the rubber. Brunella *et al.* [28] examined devulcanized ethylene propylene diene monomer (EPDM) using FTIR and other techniques with a continuous thermomechanical corotating twin-screw extruder. The efficiency of the process was found depending on the geometry of the extruder and the specific conditions of the process. Colom and coworker [29, 30] utilized FTIR to analyze the devulcanization process of GTR, identifying various mechanisms linked to the disruption of the crosslinked structure and the degradation of the sample.

This work seeks to address two different goals. First, it aims to determine the effects of thermochemomechanical treatment on the devulcanization process of GTR by combining thermochemomechanical (TM) and microwave (MW) processes as of (TM+MW) process. For the characterization of the obtained samples, FTIR, thermogravimetric analysis (TGA), and scanning electron microscopy (SEM) techniques have been used. Secondly, it aspires, through careful analysis, to utilize the mentioned techniques for monitoring the degree and nature of devulcanization attained in a given sample. The methodology is that FTIR provides information about structural changes affecting each sample based on the devulcanization process it undergoes. Additionally, using attenuated total reflectance (ATR) spectroscopy allows the investigation of chemical transformations on the material's surface, monitoring exudations of the additives incorporated into the GTR. The TGA technique allows the observation of how devulcanization affects the thermal degradation temperature (TDT), which is representative of the stability and the crosslinks present in the sample along with the amount of residue generated. SEM enabled examination of how the devulcanization process affects the surface of the samples and confirms migrations phenomena. The results obtained with these techniques are completed and/or referenced to the Horikx plot and sorption results.

2. Materials and methods

2.1. Materials

The GTR used is sourced from passenger cars with a particle size ranging from 500 to 800 μm, exhibiting a silky, powdery appearance. Passenger car tires contain more synthetic rubber (27%) than natural rubber (14%), approximately 28% carbon black, 14–15% steel, and 16–17% fiber, fillers, accelerators, antiozonants, curing additives, and other components. The exact tire composition is not known because each company keeps it confidential, leading to assumptions and average values. Table 1 displays a standard composition.

2.2. Devulcanization of GTR

Devulcanization process of GTR by combined thermochemomechanical/microwave procedures, has been carried out according to the procedure already tested and published by our group in a previous paper [24]. In summary, the thermomechanical treatment is carried out in a Brabender plastograph at 80 °C and 80 rpm for 30 min, including the addition of 2 phr of benzoyl peroxide (BPO) (devulcanizing agent) which helps the thermochemomechanical devulcanization. The microwave irradiation takes place in a prototype microwave oven with a motorized stirring adapted to our laboratory. The microwave devulcanization process was performed by setting the magnetron power to 700 W, 80 rpm of the stirrer, and 3, 6, and 9 min of MW exposure. Both processes were conducted separately and not continuously.

2.3. Measurements

The samples were subjected to Soxhlet extraction in toluene for 18 h and then dried for 12 h at 80 °C. This process separates the insoluble fraction, or gel fraction, of the rubber from the soluble fraction. A higher sol content in a devulcanizate indicates more small molecules, which improves processability and curing. The gel fraction is determined by measuring the weight of the samples before and after extraction.

To analyze the physical mechanism that takes place during the devulcanization process applied to the different samples the Horikx plot has been used [32]. The Horikx plot serves as a mathematical tool for establishing a correlation between the soluble fraction produced during the devulcanization process and the

Table 1. A standard composition of a passenger car tire [31].

Basic composition	Main compounding ingredients	Content [wt%]
Synthetic rubber	SBR, BR, Ethylene propylene rubber (EPR), silicon rubber and acrylic elastomer	51.0
Natural Rubber	Natural rubber (NR)	
Reinforcing agent	Carbon black and silica	25.0
Softener	Petroleum process oil, petroleum synthetic	19.5
Vulcanizing accelerators	Benzothiazyl Disulfide (MBTS), Dipropylene Glycol (DPG), Renogram Hexa	1.5
Vulcanizing agent	Sulphur	1.0
Vulcanizing accelerator aid	ZnO, stearic acid (StA)	0.5
Antioxidants	IPPD	1.0
Fillers	Calcium carbonate	0.5

decrease in crosslink density. This reduction may arise from the selective cleavage of the cross-links formed by –S–S– bonds (interchain bonds) or from the rupture of the main polymer chain (intrachain bonds). When main chain scission occurs (degradation), the relation between the soluble fraction of the polymer and the relative decrease in inter/intrachain bond density is given by Equation (1):

$$1-\frac{\vartheta_f}{\vartheta_i}=1-\left[\frac{\left(1-\sqrt{S_f}\right)^2}{\left(1-\sqrt{S_i}\right)^2}\right] \quad (1)$$

where S_i is the initial soluble fraction of the rubber, S_f is the soluble fraction of the sample after the process, ϑ_i is the initial cross-linking density, and ϑ_f is the cross-linking density of the sample after the treatment. For inter/intrachain bonds breakage (proper devulcanization), the soluble fraction is related to the relative decrease in cross-link density according to Equation (2):

$$1-\frac{\vartheta_f}{\vartheta_i}=1-\left[\frac{\gamma_f\left(1-\sqrt{S_f}\right)^2}{\gamma_i\left(1-\sqrt{S_i}\right)^2}\right] \quad (2)$$

where the parameters γ_f and γ_i called cross-linking indexes, are the average numbers of crosslinked units per chain before and after treatment, respectively. The cross-linking indexes are calculated from M_n and the determined crosslink density as described by Simon and Bárány [17] and Verbruggen *et al.* [33] according to Equation (3):

$$\gamma_x=\vartheta_x\frac{M_n}{\rho} \quad (3)$$

where γ_x is the cross-linking index, ϑ_x [mol/dm^3] is the cross-link density, M_n [g/mol] is the number-average molecular weight of the rubber and ρ is the density of the rubber [g/dm^3].

Cross-linking density refers to presence of crosslinks inside the specimen. The ASTM D297/13 test involves exposing the samples to a solvent, toluene, which causes the sample to swell by penetrating the spaces within the crosslinked clusters.

Before swelling, the test requires a preliminary extraction with acetone to remove low molecular weight substances and facilitate the subsequent penetration of toluene. The crosslinking density of the samples was then determined by equilibrium swelling in toluene (at room temperature (*RT*) for 72 h, followed by drying to constant mass at 70 °C), according to the Flory-Rehner Equation (4) [20]:

$$V_e=\frac{-\ln\left(1-V_r\right)+V_r+\chi V_r^2}{V_1\left(\sqrt[3]{V_r}-\frac{V_r}{2}\right)} \quad (4)$$

where V_e is cross-link density [mol/cm^3]; V_1 is the molar volume of solvent-toluene (106,13 cm^3/mol); χ is the rubber-solvent interaction parameter (0,39), and V_r means volume fraction of rubber in the swollen sample, which is calculated by using the Ellis and Welding equation (Equation (5)):

$$V_r=\frac{\frac{m_r}{\rho_r}}{\frac{m_r}{\rho_r}+\frac{m_s}{\rho_s}} \quad (5)$$

where m_s is the mass of the swollen rubber sample [g], m_r is the mass of the dry rubber sample [g] (24 h at *RT*), ρ_s is the density of the solvent, toluene (0,8669 g/cm^3), and ρ_r is the density of rubber sample.

The chemical structure of devulcanized GTR was determined using FTIR-ATR analysis performed by means of a Spectrum Two spectrometer from Perkin Elmer (USA). The device had an ATR attachment with a diamond crystal. Spectra were registered at 2 cm^{-1} resolution and 40 scans in the range of 3500–500 cm^{-1}, in which the compound signals related to different deformation bands can be observed.

TGA was performed on a Perkin Elmer TGA 8000 apparatus (USA). GTR samples weighing approximately 10 mg were placed in a corundum dish. The measurement was conducted in the temperature range 30–800 °C and under oxidant atmosphere (air) (30 ml/min), at a heating rate of 20 °C/min. The obtained results are the average of three measurements per sample.

The morphology of GTR surfaces was observed with a JEOL 5610 scanning electron microscope (Japan). Before observation, the samples were covered with a fine gold-palladium layer to increase their conductivity in a vacuum chamber.

The sorption isotherms were carried out at room temperature (25 °C), by contacting, in an Erlenmeyer flask, 2 g of GTR with 40 ml of solution of a given concentration of acetic acid in the range of 0.05 to 0.5 M. The Erlenmeyer flask was kept stirring at 50 rpm for 120 min to reach equilibrium, a value obtained from the kinetic experiments [34]. After this

time, the mixtures were filtered and the concentration of acetic acid in such solution was determined by titration with 0.1 M KOH. The assays were performed in duplicate. The experimental results obtained for the GTR were adjusted to the Freundlich isotherms, which in their linearized form are described by Equation (6):

$$\log q_e = \log k_F + \frac{1}{n}\log C_e \quad (6)$$

where q_e is the equilibrium concentration of sorbate (HAc) per unit mass of sorbent (GTR) [mol/g]; C_e is the equilibrium concentration of adsorbate in the residual solution [mol/l]; k_F and n are constants. k_F is linked to absorbent efficiency, and n is linked to the speed at which the sorbent absorbs the sorbate.

3. Results and discussion

3.1. Infrared analysis

The spectra in Figure 1 (spectral range 1700–1300 cm^{-1}) show bands at 1638 and 1596 cm^{-1} assigned to the antioxidant *N*-isopropyl-*N*′-phenyl-*p*-phenylenediamine (IPPD) [30]. The devulcanization process induces chain breakage within the GTR structure, thereby facilitating the migration of additives from the inner to the surface of the sample.

The bands assigned to the IPPD present on the surface of the sample are related to this migration process that results in an exudation phenomenon causing the growth of the band at 1638 cm^{-1}. In the same way, the bands at 1537 and 1530 cm^{-1} assigned to zinc stearate ($ZnSt_2$) exhibit considerable change. When the samples are submitted to the devulcanization process from 3 to 9 min in MW, the 1530 cm^{-1} band increases. The migration of the $ZnSt_2$ molecules, which is also related to the physicochemical interaction with the devulcanized samples compared to the non-devulcanized GTR samples, has also been observed in thermoplastic blends [35].

The 1445 cm^{-1} band, attributed to methylene groups ($–CH_2–$), experiences a decrease as the devulcanization process intensifies, indicating the cleavage of rubber chains [20]. Meanwhile, the 1417 cm^{-1} band, assigned to the (–CH=CH–) group, intensified during the devulcanization process. This increase may be attributed to the formation of unsaturated chains caused by devulcanization itself and/or other degradation phenomena. The 1373 and 1364 cm^{-1} bands, assigned to the methyl group ($–CH_3$), increase with the devulcanization process due to thermooxidation that leads to Norrish reactions types I and II, involving the cleavage of the rubber polymeric chain and the formation of methyl groups [36].

A careful study of the FTIR bands offers deeper insight into the phenomena that take place in the samples submitted to MW devulcanization. Figure 2 shows several band variations in the 1270–540 cm^{-1} spectral range. The SiO_2 remains chemically stable regardless of the devulcanization process, and we can consider the 1075 cm^{-1} band associated with this compound as a reference [20]. This band presents a shoulder due to a peak overlapped with surrounding bands located at 1025 cm^{-1} that is assigned to the carbon black (CB) present in the samples. This band decreases when the reference GTR sample is submitted to MW treatment for 3 and 6 min due to the formation of CO_2, but if the MW exposure reaches 9 min, part of the sample carbonizes, increasing the total content CB. This appears in the FTIR as a double peak constituted by the SiO_2 and CB bands [36, 37].

The vibration modes appearing at 963 and 908 cm^{-1} are assigned to the trans group –CH=CH– and the CH_2 of butyl rubber (BR), respectively [38, 39]. These bands decrease depending on the devulcanization

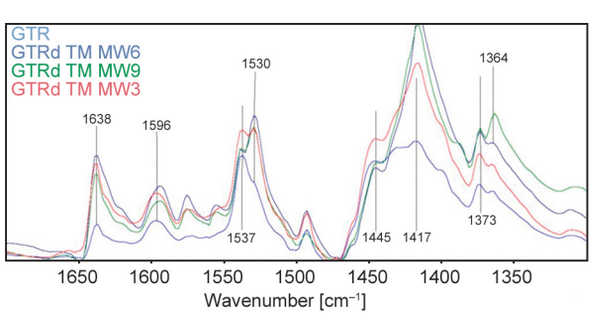

Figure 1. FTIR spectral range 1700–1300 cm^{-1} of GTR samples subjected to 3, 6 and 9 min of microwave treatment. Absorbance in arbitrary units.

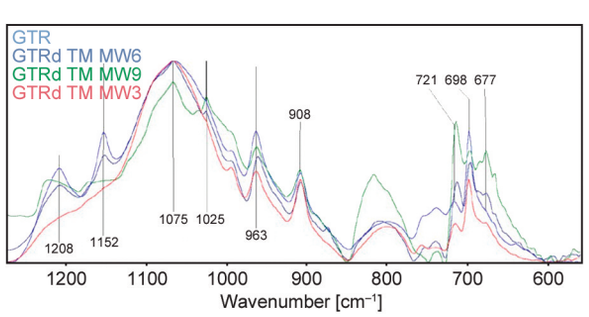

Figure 2. FTIR spectral range 1270–540 cm^{-1} of GTR samples subjected to 3, 6 and 9 min of microwave treatment. Absorbance in arbitrary units.

process. This decrease is due to the breakage of the macromolecular chain that has taken place during the thermochemomechanical (TM) process. A decrease in the 698 cm^{-1} band assigned to the CH of the aromatic ring of SBR [40] is also observed, which can be associated with the degradation of the phenyl group during the thermomechanical devulcanization process [41]. The 721 cm^{-1} band assigned to unsaturations in cis configurations increases with the treatment process. The band at 677 cm^{-1} attributed to the C–SH group increases when the devulcanization process is intense, which implies that there is a sulfur breakdown with the formation of the sulfhydryl group (C–SH) [42].

The spectra in Figure 3 allow us to discern the differences between the devulcanization process with only employing microwaves (MW) and the combined TM/MW devulcanization process. Significant spectral differences are observed between both types of devulcanization, among which it is worth highlighting: i) short-range displacements in the bands of 1537–1530, 1450–1443, 1415–1410 and 1384–1373 cm^{-1}; ii) decrease in the bands at 1208, 1153 and 1078 cm^{-1} iii) appearance of the 1021 cm^{-1} band.

The band observed in the samples devulcanized with the combined process (TM/MW) is attributed to $ZnSt_2$. As mentioned previously, the increase in this band and a displacement to 1530 cm^{-1} is due to the exudation of the $ZnSt_2$. The physicochemical interactions of this molecule with the devulcanized samples have an influence on the wavenumber of vibration. The shift in the wavenumber suggests that there are structural differences between the samples devulcanized with thermochemomechanical (TM) and those with only microwaves (MW), resulting in distinct interactions with the $ZnSt_2$.

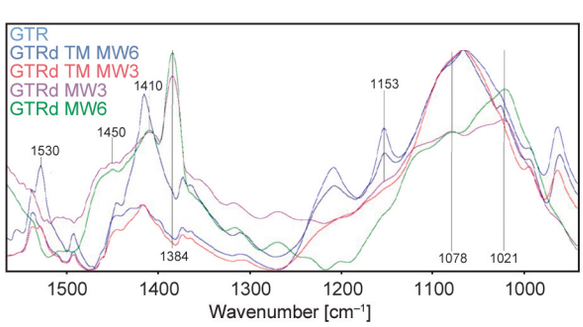

Figure 3. FTIR spectral range 1550–940 cm^{-1} of GTR samples subjected to 3 and 6 min of microwave (MW) treatment, and 3 and 6 min of thermochemomechanical/microwave (TM/MW) treatment. Absorbance in arbitrary units.

The band observed at 1450 cm^{-1} is attributed to the stretching of the $–CH_2–$ group which is characteristic of the GTR elastomers (NR, SBR, BR). The combined treatment (TM/MW) shifts the band from 1450 to 1443 cm^{-1}. The $–CH_2–$ band appears at a wavenumber that is the combination of the vibrations of this group in the different elastomers present in the sample. The shift in the wavenumber can be associated with the differences in the effect of the treatment on the elastomers involved. If the TM treatment affects more one type of elastomer than the other, the $–CH_2–$ group of this elastomer will show a decrease in its absorption. Since not all the $–CH_2–$ groups in the several present elastomers vibrate at exactly the same number, the result is a displacement of the average wavenumber of the total band.

The band at 1410 cm^{-1} assigned –C=C–H in plane C–H bend increases significantly with devulcanization with MW, likewise the combined treatment shifts this band to 1415 cm^{-1}. The band of 1384 cm^{-1}, assigned to $–CH_3$ symmetric bend increases significantly with devulcanization with MW. These changes can be rationalized similarly to the case of the $–CH_2–$ groups, considering the variations induced by the type of treatment on different polymers, or alternatively, by the diverse outcomes obtained from the thermochemomechanical (TM) and microwave (MW) processes.

The region including the 1078 and the 1021 cm^{-1} bands assigned to SiO_2 and carbon black (CB) respectively show differences according to the treatment used. The samples devulcanized with the combined treatment TM/MW are subjected to greater mechanical friction that disperses the CB generated by the MW process. Likewise, the TM treatment opens the macromolecular structure and favors the movement of SiO_2. These changes imply differences in the intensity of these bands and modify the shape of the spectra in that region.

3.2. Thermal analysis

Figure 4 shows the differential thermogravimetric shows the derivative thermogravimetric analysis (DTGA) conducted on samples. Overall, there is an obvious change in DTG curves of samples with respect to the reference one in view of transitional change from a curve showing a peak followed by an intensified shoulder at higher temperatures (reference sample) to bimodal curves (particularly in the case

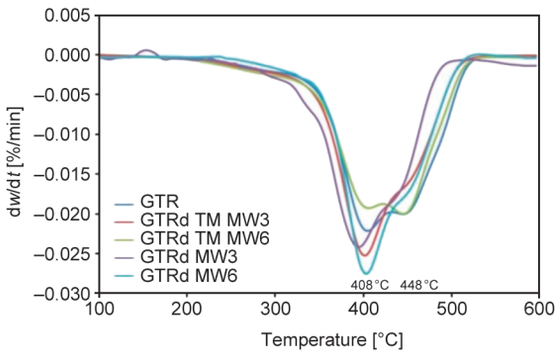

Figure 4. DTG corresponding to the reference GTR sample and the devulcanized samples.

of GTR TM MW6 sample). The reference sample presents the characteristic peak of NR at 408 °C followed by a second peak at 448 °C, which can be ascribed to the presence of a mixture of synthetic rubber (SBR, BR) [43]. The results show that samples subjected to a combined TM/MW devulcanization process underwent more pronounced degradation than the ones processed only with MW. Correspondingly, a decrease in the thermal decomposition temperature (TDT) from 408 to 393 °C alongside an improved structural homogenization of the sample can be considered. The homogenization is signaled by the smoothing and the narrowness of the DTG curve and the quite complete disappearance of the peak corresponding to the synthetic components (448 °C).

Samples treated with MW for 3 min retain the structure of natural rubber (NR) and synthetic elastomers to some extent. The MW treatment primarily targets the weaker –S–S– bonds. Conversely, treatment with MW for 6 min results in additional degradation of the structure of synthetic elastomers, depressing their thermal decomposition temperature from 408 to 402 °C. It can be seen that the GTR TMMW6 sample shows a secondary degradation peak rather than the shoulder observed for GTR TMMW3, which outlines the role of treatment time. Moreover, a combination of TM and MW processes intensified the secondary degradation stage, which is a signature of successful devulcanization methodology. This observation is coherent with the FTIR results presented previously, indicating carbonization of a portion of the polymeric structure with longer MW treatment periods.

3.3. Physical analysis by Horikx plot

The Horikx equations provide interesting information relating to the soluble fraction generated after the devulcanization process of the GTR samples and the relative decrease in the cross-linking density. The main purpose is to discern between the decrease of crosslinking resulting from the cleavage of the main polymeric chain and the breaking of the S–S bonds linking elastomeric chains.

According to Horikx's postulates, the values that are comprised between the lines of main chain breakage and S–S bond breakage have undergone a proper devulcanization process. The samples situated close to the upper line have been more affected by the breaking of the main polymeric chain and are consequently more degraded. On the contrary, the samples closer to the lower line are more prone to S–S cross-linking breakage which would be considered a proper theoretical devulcanization process.

Figure 5 illustrates the positioning of the examined samples on the Horikx plot. It is observed that all samples have undergone devulcanization, resulting in a decrease in crosslinking density. However, not all samples exhibit the same degree of devulcanization, and the manner in which crosslinking density decreases varies qualitatively depending on the type and duration of treatment.

Samples subjected to thermochemomechanical (TM) treatment show a higher degradation of the main polymeric chain, generally aligning closer to the upper line on the plot. The overall greater intensity of TM treatment, has been discussed previously as a typical feature. However, the Horikx plot indicates that the decrease in crosslinking primarily occurs through the cleavage of the main –C–C– chain, which may not be advantageous for many applications.

On the other hand, samples treated with microwaves (MW) experience a reduction in crosslinking density more closely related to the scission of –S–S– bonds. The selectivity of the MW process is higher than that of TM and can be more effectively focused

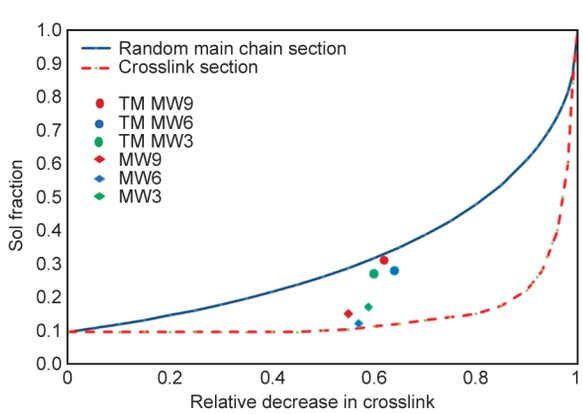

Figure 5. Horikx plot of sol fraction of devulcanized samples.

on breaking the –S–S– bonds while leaving the –C–C– bonds of the proper polymeric chain mainly unaffected.

Following the same rationale, the combination of TM/MW results in a higher degree of devulcanization compared to using only MW. In the TM/MW process, the highest devulcanization value achieved is 64%, attained with 6 minutes of MW treatment. In contrast, when utilizing only 6 min of MW treatment, a devulcanization of only 59% is achieved.

3.4. Microstructural analysis

Figure 6 depicts SEM microphotographs of the samples. The untreated GTR sample exhibits a homogeneous, rough surface with visible particles which, by their shape and number, are probably silica. In contrast, the samples devulcanized with MW display a distinct morphology, characterized by nodules and the presence of particles that are, according to similar images, related to $ZnSt_2$ formed during the vulcanization process, which are observed on the surface due to exudation.

The samples subjected to the combined TM/MW devulcanization process are more heterogeneous, with a greater amount of $ZnSt_2$ and SiO_2 particles and a greater presence of voids. This is because the combined process, as evidenced by the TGA analyses, significantly degrades the GTR samples.

3.5. Sorption analysis

Chemical characterization was conducted to characterize the devulcanization process and its structural changes by analyzing the sorption capacity of each of the different samples.

For this characterization, it has been observed that the Freundlich isotherm provides the best fit. The experimental data were fitted to the Freundlich model to quantify the behavior of the various samples. The best-fitting results correspond to the sample GTR MW3 ($R^2 > 0.97$), obtaining the model parameters (k_F and n) indicated in Table 2. The Freundlich model accepts that the limiting stage of sorption is chemisorption, which involves the interactions between the ionic centers of the sorbent (*e.g.*, COO–) and H^+ ions. The most common thing is that the sorption process takes place through the different London forces that are generated inside the devulcanized GTR. As observed through the SEM microphotographs, the devulcanization process generates a significant amount of microporosities and voids that allow organic compounds to lodge.

As seen in Table 2, the values of k_F and n are different for each of the samples. The k_F values linked to the efficiency of the sorbent indicate that the combined TM/MW treatment gives better results than the reference sample and the sample treated only with MW. The thermochemomechanical devulcanization process combined with microwave opens the structure of the samples, thereby increasing the sorption capacity on the sorbent (*i.e.*, from 0.0017 for the GTR to 0.0025 for GTR TMMW3). These results are in accordance with the several aspects discussed previously.

4. Conclusions

As previously stated, this paper pursues two distinct objectives. Firstly, it seeks to elucidate the differences produced in the samples by the two types of devulcanization processes (TM/MW and MW). Secondly, it aims to provide a roadmap for essential points to consider when monitoring these processes by FTIR, DTGA, SEM with the complement of the Horikx plot and the sorption studies.

In relation to the vulcanization processes, various tests demonstrate that, as expected, the combined TM/MW treatment induces more bond scission compared to the MW treatment alone. At the same time, the MW treatment is more selective than the thermochemomechanical. While the MW treatment selectively targets the –S–S– bonds, leading to effective devulcanization, the TM/MW treatment acts indiscriminately on both the –S–S– and –C–C bonds. These conclusions are supported by the differences that appear in the FTIR spectra, the analysis of the

Table 2. Parameters corresponding to Freundlich isotherm.

Sample	k_F	n	Freundlich isotherm	Regression coefficient
GTR	0.00170	1.048	$y = 0.95x - 2.77$	0.861
GTR MW3	0.00140	1.190	$y = 0.84x - 2.84$	0.972
GTR MW6	0.00240	1.149	$y = 0.87x - 2.62$	0.940
GTR TMMW3	0.00250	2.040	$y = 0.49x - 3.34$	0.951
GTR TMMW6	0.00204	1.298	$y = 0.77x - 2.69$	0.885

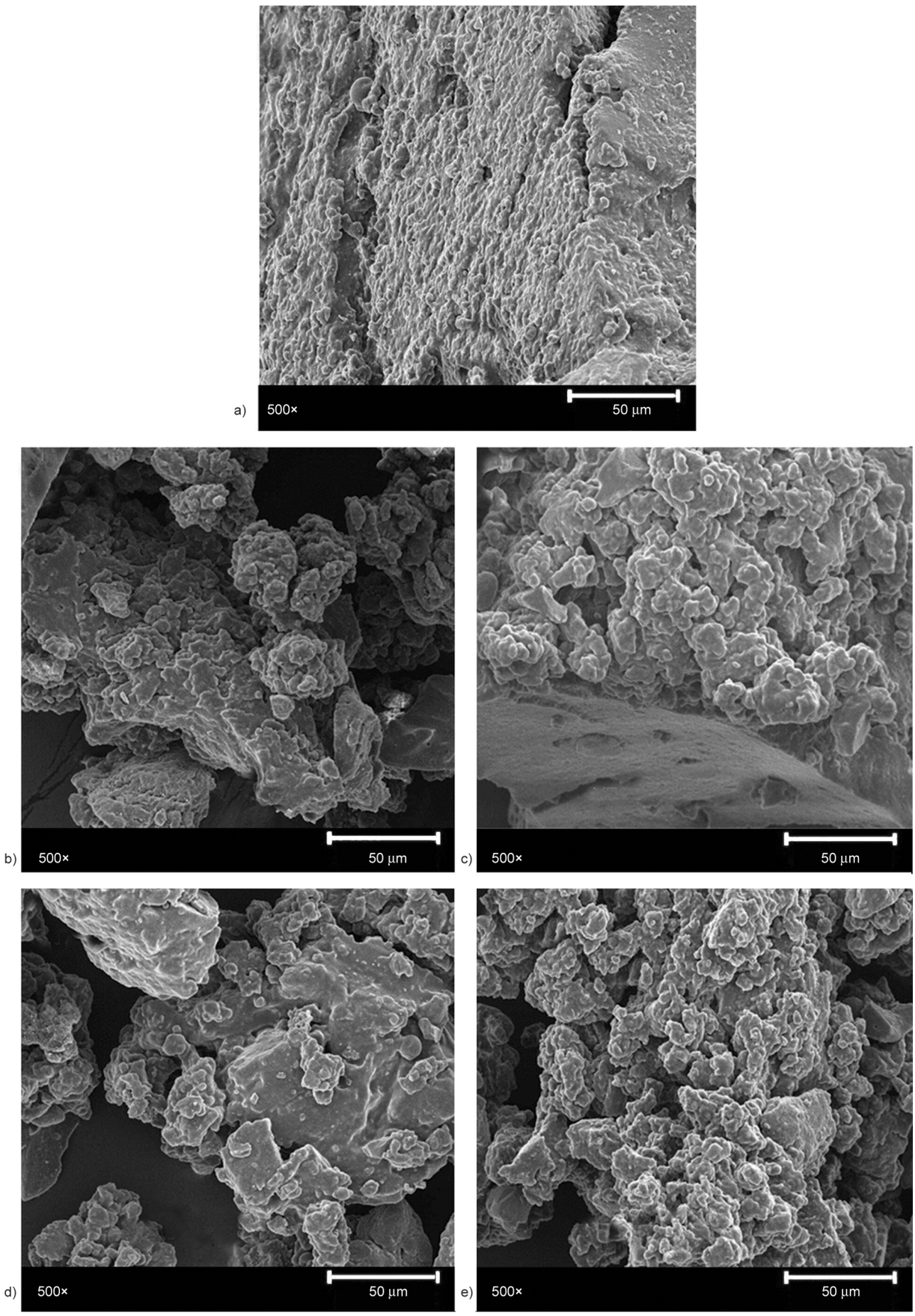

Figure 6. GTR samples obtained by SEM. Where a) sample without devulcanization; b) sample devulcanized by treatment with MW for 3 min; c) sample devulcanized by treatment with MW for 6 min; d) sample devulcanized by combined treatment TMMW3 and e) sample devulcanized by combined treatment TM/MW 6 min (magnification 500×).

DTGA results, the positioning of the samples in the Horikx graphics, SEM observations, and sorption studies.

The analysis of the FTIR spectra reveals key bands and changes associated with the alterations experienced by the samples during the devulcanization process. Some interesting phenomena that can be monitored with this technique include the migration of antioxidants and zinc stearate, the decrease in methylene groups ($–CH_2–$), which indicates the cleavage of rubber chains, and the formation of unsaturated bonds caused by devulcanization and other degradation processes. There is also an increase in methyl groups ($–CH_3$) due to chain scission and various types of degradation.

The results of the thermal analysis show that, as mentioned previously, the samples subjected to a combined TM/MW devulcanization process suffer more pronounced degradation than the ones treated only with MW. This is evidenced by a decrease in the thermal decomposition temperature (TDT) from 408 to 393 °C.

The DTGA also shows that samples treated with MW for 3 min retain the structure of natural rubber (NR) and synthetic elastomers to some extent, while treatment with MW for 6 min or more results in additional degradation of the structures.

The Horikx plot allows us to verify that all samples have undergone devulcanization. Samples subjected to thermochemomechanical (TM) treatment show a higher degradation of the main polymeric chain, and samples treated with microwaves (MW) experience a reduction in crosslinking density more closely related to the scission of –S–S– bonds.

The SEM and sorption analysis confirm the results obtained previously.

Acknowledgements

We appreciate the collaboration and work carried out by Robert Blazquez and Patricia Muñoz. This publication is a part of grant PID2021-126165OB-I00 founded by MCIN/AEI/10.13039/501100011033 and by ERDF, A Way of Making Europe by the European Union.

References

[1] Goevert D.: The value of different recycling technologies for waste rubber tires in the circular economy – A review. Frontiers in Sustainability, **4**, 1282805 (2024). https://doi.org/10.3389/frsus.2023.1282805

[2] Wagner S., Klöckner P., Reemtsma T.: Aging of tire and road wear particles in terrestrial and freshwater environments – A review on processes, testing, analysis and impact. Chemosphere, **288**, 132467 (2022). https://doi.org/10.1016/j.chemosphere.2021.132467

[3] Hagelüken C., Goldmann D.: Recycling and circular economy – Towards a closed loop for metals in emerging clean technologies. Mineral Economics, **35**, 539–562 (2022). https://doi.org/10.1007/s13563-022-00319-1

[4] Wiśniewska P., Haponiuk J. T., Colom X., Saeb M. R.: Green approaches in rubber recycling technologies: Present status and future perspective. ACS Sustainable Chemistry and Engineering, **11**, 8706–8726 (2023). https://doi.org/10.1021/acssuschemeng.3c01314

[5] Araujo-Morera J., Verdejo R., López-Manchado M. A., Santana M. H.: Sustainable mobility: The route of tires through the circular economy model. Waste Management, **126**, 309–322 (2021). https://doi.org/10.1016/j.wasman.2021.03.025

[6] Ghowsi M. A., Jamshidi M.: Recycling waste nitrile rubber (NBR) and improving mechanical properties of re-vulcanized rubber by an efficient chemo-mechanical devulcanization. Advanced Industrial and Engineering Polymer Research, **6**, 255–264 (2023). https://doi.org/10.1016/j.aiepr.2023.01.004

[7] Chittella H., Yoon L. W., Ramarad S., Lai Z-W.: Rubber waste management: A review on methods, mechanism, and prospects. Polymer Degradation and Stability, **194**, 109761 (2021). https://doi.org/10.1016/j.polymdegradstab.2021.109761

[8] Ghosh J., Hait S., Ghorai S., Mondal D., Wießner S., Das A., De D.: Cradle-to-cradle approach to waste tyres and development of silica based green tyre composites. Resources, Conservation and Recycling, **154**, 104629 (2020). https://doi.org/10.1016/j.resconrec.2019.104629

[9] Costamagna M., Brunella V., Luda M. P., Baricco M., Romagnolli U., Muscato B., Girotto M., Baricco M., Rizzi P.: Environmental assessment of rubber recycling through an innovative thermo-mechanical devulcanization process using a *co*-rotating twin-screw extruder. Journal of Cleaner Production, **348**, 131352 (2022). https://doi.org/10.1016/j.jclepro.2022.131352

[10] Pirityi D. Z., Pölöskei K.: Thermomechanical devulcanisation of ethylene propylene diene monomer (EPDM) rubber and its subsequent reintegration into virgin rubber. Polymers, **13**, 1116 (2021). https://doi.org/10.3390/polym13071116

[11] Seghar S., Asaro L., Rolland-Monnet M., Hocine N. A.: Thermo-mechanical devulcanization and recycling of rubber industry waste. Resources, Conservation and Recycling, **144**, 180–186 (2019). https://doi.org/10.1016/j.resconrec.2019.01.047

[12] Mangili I., Lasagni M., Anzano M., Collina E., Tatangelo V., Frazetti A., Caracino P., Isayev A. I.: Mechanical and rheological properties of natural rubber compounds containing devulcanized ground tire rubber from several methods. Polymer Degradation and Stability, **121**, 369–377 (2015). https://doi.org/10.1016/j.polymdegradstab.2015.10.004

[13] Mangili I., Lasagni M., Huang K., Isaye A. I.: Modeling and optimization of ultrasonic devulcanization using the response surface methodology based on central composite face-centered design. Chemometrics and Intelligent Laboratory Systems, **144**, 1–10 (2015). https://doi.org/10.1016/j.chemolab.2015.03.003

[14] Cataldo F.: Chemochemistry of sulfur-based vulcanization and of devulcanized and recycled natural rubber compounds. International Journal of Molecular Sciences, **24**, 2623 (2023). https://doi.org/10.3390/ijms24032623

[15] Wiśniewska P., Wang S., Formela K.: Waste tire rubber devulcanization technologies: State-of-the-art, limitations and future perspectives. Waste Management, **150**, 174–184 (2022). https://doi.org/10.1016/j.wasman.2022.07.002

[16] Hejna A., Korol J., Przybysz-Romatowska M., Zedler Ł., Chmielnicki B., Formela K.: Waste tire rubber as low-cost and environmentally-friendly modifier in thermoset polymers – A review. Waste Management, **108**, 106–118 (2020). https://doi.org/10.1016/j.wasman.2020.04.032

[17] Simon D. A., Bárány T.: Microwave devulcanization of ground tire rubber and its improved utilization in natural rubber compounds. ACS Sustainable Chemistry and Engineering, **11**, 1797–1808 (2023). https://doi.org/10.1021/acssuschemeng.2c05984

[18] Molanorouzi M., Mohaved S. O.: Reclaiming waste tire rubber by an irradiation technique. Polymer Degradation and Stability, **128**, 115–125 (2016). https://doi.org/10.1016/j.polymdegradstab.2016.04.001

[19] Formela K., Hejna A., Zedler Ł., Colom X., Cañavate J.: Microwave treatment in waste rubber recycling – Recent advances and limitations. Express Polymer Letters, **13**, 565–588 (2019). https://doi.org/10.3144/expresspolymlett.2019.48

[20] Colom X., Faliq A., Formela K., Cañavate J.: FTIR spectroscopic and thermogravimetric characterization of ground tyre rubber devulcanized by microwave treatment. Polymer Testing, **52**, 200–208 (2016). https://doi.org/10.1016/j.polymertesting.2016.04.020

[21] Li X., Xu X., Liu Z.: Cryogenic grinding performance of scrap tire rubber by devulcanization treatment with $ScCO_2$. Powder Technology, **374**, 609–617 (2020). https://doi.org/10.1016/j.powtec.2020.07.026

[22] Allan K. M., Bedzo O. K. K., van Rensburg E., Görgens J. F.: The microbial devulcanisation of waste ground tyre rubber using *At. ferrooxidans* DSMZ 14,882 and an unclassified sulphur-oxidising consortium. Waste and Biomass Valorization, **12**, 6659–6670 (2021). https://doi.org/10.1007/s12649-021-01468-0

[23] Saputra R., Walvekar R., Khalid M., Mubarak N. M., Sillanpää M.: Current progress in waste tire rubber devulcanization. Chemosphere, **265**, 129033 (2021). https://doi.org/10.1016/j.chemosphere.2020.129033

[24] Colom X., Cañavate J., Formela K., Shadman A., Saeb M. R.: Assessment of the devulcanization process of EPDM waste from roofing systems by combined thermomechanical/microwave procedures. Polymer Degradation and Stability, **183**, 109450 (2021). https://doi.org/10.1016/j.polymdegradstab.2020.109450

[25] Simon D. Á., Bárány T.: Effective thermomechanical devulcanization of ground tire rubber with a *co*-rotating twin-screw extruder. Polymer Degradation and Stability, **190**, 109626 (2021). https://doi.org/10.1016/j.polymdegradstab.2021.109626

[26] de Sousa F. D. B., Zanchet A., Scuracchio C. H.: Influence of reversion in compounds containing recycled natural rubber: In search of sustainable processing. Journal of Applied Polymer Science, **134**, 45325 (2017). https://doi.org/10.1002/app.45325

[27] Paulo G. D., Hirayama D., Saron C.: Microwave devulcanization of waste rubber with inorganic salts and nitric acid. Advanced Materials Research, **418–420**, 1072–1075 (2011). https://doi.org/10.4028/www.scientific.net/AMR.418-420.1072

[28] Brunella V., Aresti V., Romagnolli U., Muscato B., Girotto M., Rizzi P., Luda M. P.: Recycling of EPDM *via* continuous thermo-mechanical devulcanization with *co*-rotating twin-screw extruder. Polymers, **14**, 4853 (2022). https://doi.org/10.3390/polym14224853

[29] Colom X., Marín-Genesca M., Mujal R., Formela K., Cañavate J.: Structural and physico-mechanical properties of natural rubber/GTR composites devulcanized by microwaves: Influence of GTR source and irradiation time. Journal of Composite Materials, **52**, 3099–3108 (2018). https://doi.org/10.1177/0021998318761554

[30] Colom X., Andreu-Mateu F., Cañavate F. J., Mujal R., Carrillo F.: Study of the influence of IPPD on thermo-oxidation process of elastomeric hose. Journal of Applied Polymer Science, **114**, 2011–2018 (2009). https://doi.org/10.1002/app.30746

[31] Pehlken A., Essadiqi E.: Scrap tire recycling in Canada. CANMET Materials Technology Laboratory. Ottawa (2005). https://doi.org/10.13140/2.1.1941.8400

[32] Horikx M. M.: Chain scissions in a polymer network. Journal of Polymer Science, **19**, 445–454 (1956). https://doi.org/10.1002/pol.1956.120199305

[33] Verbruggen M. A. L., van der Does L., Noordermeer J. W. M., van Duin M., Manuel H. J.: Mechanisms involved in the recycling of NR and EPDM. Rubber Chemistry and Technology, **72**, 731–740 (1999). https://doi.org/10.5254/1.3538830

[34] Casadesús M., Álvarez M. D., Macanás J., Colom X., Cañavate J., Garrido N., Molins G., Carrillo F.: Use of keratinous residues for copper sorption in aqueous solution (in Spanish). AFINIDAD, **589**, 13–21 (2019).

[35] Cañavate J., Carrillo F., Casas P., Colom X., Suñol J. J.: The use of waxes and wetting additives to improve compatibility between HDPE and ground tyre rubber. Journal of Composite Materials, **44**, 1233–1245 (2010). https://doi.org/10.1177/0021998309351602

[36] Chen J., Hu M., Li Y., Li R., Qing L.: Significant influence of bound rubber thickness on the rubber reinforcement effect. Polymers, **15**, 2051 (2023). https://doi.org/10.3390/polym15092051

[37] Chen J., Hu M-Y., Qing L., Liu P., Li L., Li R., Yue C-X., Lin J-H.: Study on boundary layer and surface hardness of carbon black in natural rubber using atomic force microscopy. Polymers, **14**, 4642 (2022). https://doi.org/10.3390/polym14214642

[38] Schnabel W.: Polymer degradation: Principles and practical applications. Hanser, München (1992).

[39] Brazier D. W., Nickel G. H.: Thermoanalytical methods in vulcanizate analysis II. Derivative thermogravimetric analysis. Rubber Chemistry and Technology, **48**, 661–667 (1975). https://doi.org/10.5254/1.3539668

[40] Hummel D. O.: Infrared analysis of polymers, resins and additives: An atlas. Vol. I, Plastics, elastomers, fibers and resins. Part 1: Text. Wiley, New York (1971).

[41] Vesel A., Zaplotnik R., Primc G., Mozetič M.: Evolution of surface functional groups and aromatic ring degradation upon treatment of polystyrene with hydroxyl radicals. Polymer Degradation and Stability, **218**, 110582 (2023). https://doi.org/10.1016/j.polymdegradstab.2023.110582

[42] Bower D. I., Maddams W. F.: The vibrational spectroscopy of polymers. Cambridge University Press, Cambridge (1989).

[43] Datta S., Antos J., Stocek R.: Characterisation of ground tyre rubber by using combination of FT-IR numerical parameter and DTG analysis to determine the composition of ternary rubber blend. Polymer Testing, **59**, 308–315 (2017). https://doi.org/10.1016/j.polymertesting.2017.02.019